Fusion and reaction mechanism evolution in ^{24}Mg+ ^{12}C at intermediate energies

M. Samri,[1,*] F. Grenier,[2] G. C. Ball,[3,†] L. Beaulieu,[2,‡] L. Gingras,[2,‡] D. Horn,[3] Y. Larochelle,[2,§] R. Moustabchir,[2] R. Roy,[2] C. St-Pierre,[2] and D. Theriault[2]

[1]*Laboratoire de Physique Nucléaire et Applications, Université Ibn Tofail, Kénitra, Morocco*

[2]*Laboratoire de Physique Nucléaire, Département de Physique, de Génie physique et d'Optique,
Université Laval, Québec, Canada G1K 7P4*

[3]*AECL, Chalk River Laboratories, Chalk River, Ontario, Canada K0J 1J0*

The formation and deexcitation of fusionlike events selected in events with a total charge equal or greater than 16 in ^{24}Mg+ ^{12}C system has been investigated at 25, 35, and 45 MeV/nucleon with a large multidetector array. Central single-source events are selected by use of the statistical discriminant analysis method applied to a set of 26 global variables. The fusion cross section has been extracted for the three bombarding energies and compared to other experimental data and to theoretical predictions. The total multiplicity is found to first increase to a maximum value and then decrease with increasing beam energy. It is shown that this behavior is connected to the opening of multifragmentation channels at 45 MeV/nucleon and the disappearance of channels with only light charged particles.

The decay by emission of intermediate mass fragments (IMF's) of excited nuclear systems formed in intermediate energy heavy-ion reactions, linked to the so-called multifragmentation decay mode, has been the subject of many experimental and theoretical intensive studies [1,2]. This phenomenon can be studied in the decay of excited quasiprojectiles and quasitargets formed in dissipative binary-type reactions, in excited quasiprojectiles formed in peripheral reactions or in well selected ''single-source'' or fusionlike events. In this paper devoted to the ^{24}Mg+ ^{12}C system at 25, 35, and 45 MeV/nucleon, we will select fusionlike events by applying the discriminant analysis method, which has been previously used succesfully for this purpose [3,4]. This system has been the subject of an earlier work in which Larochelle *et al.* [5] have studied the dissipative binary nature of the reactions at 25 and 35 MeV/nucleon. The present analysis follows a recent study of this system in which we have focused on the experiment at 45 MeV/nucleon [4].

The experiments have been performed at the tandem accelerator superconducting cyclotron facility at Chalk River by using a ^{24}Mg beam accelerated at 25, 35, and 45 MeV/ nucleon and bombarding a 2.4 mg/cm^2 carbon target. The charged reaction products were detected in the CRL-Laval array composed of 80 detectors and covering angles in the laboratory frame from 6.8° to 46°. The set of detectors was disposed on five rings concentric on the beam direction, each ring being composed of 16 detectors. The first three rings ($6.8° < \theta_{lab} < 24°$) are each made of fast-slow phoswich de-

tectors with detection thresholds of 7.5A MeV for hydrogens and 17.6A MeV for $Z=10$ fragments. The fourth and fifth rings ($24° < \theta_{lab} < 46°$) are made of CsI(Tl), achieving isotopic resolution for $Z=1$ and 2 particles. The events were recorded on an event-by-event basis when at least three detectors were fired. The energy calibration of the detectors is accurate to about $\pm 5\%$. The present analysis is restricted to events selected in the off-line analysis to a total detected charge equal or greater than 16 which represents almost 90% of the total charge of the system.

In order to select single-source events, we have used the discriminant analysis method. This technique, mainly devoted to predict source origin, is based on a linear combination of observed characteristics that may be the multidimensional moments [3,6] or a set of global variables. In the present work, we have used a large number of global variables taking account of different aspects such as the detection, the kinematics of the reaction, the completeness of the event, and the form of the event in different frames. These variables are the total multiplicity, the light charged ($Z=1,2$) particle multiplicity, the intermediate mass fragment ($3 \leq Z \leq 9$) multiplicity, the mean of the charge distribution, the charge asymmetry [4], the maximum charge of the event, the charge and energy in the lab frame of the biggest IMF, the $Y33$ (minimum and maximum) relative velocity between particles taken three by three [7,8], the total momentum, the reconstructed center-of-mass (c.m.) velocity, the total energy in the c.m. frame, the Fox moment of order 2 H_2 [9], the product of the eigenvalues [10] of the kinetic flow tensor [11], the sphericity and coplanarity [11], the transverse energy, the anisotropy ratio [12], and the total transverse and parallel momentum. The last four quantities are calculated in both the c.m. frame and the ellipsoid frame. The flow angle, which is defined as the angle between the ellipsoid major axis corresponding to the highest eigenvalue of the kinetic energy tensor and the beam axis, is another important global variable used in many works to separate the different sources. In this work, this variable has been kept as an inde-

---

*Corresponding author. Email address: msamri@phy.ulaval.ca

†Present address: TRIUMF, 4004 Wesbrook Mall, Vancouver, BC, Canada V6T 2A3.

‡Present address: Département de Radio-Oncologie, Hôtel-Dieu, 1 rue Collins, Québec, Canada G1R 4J1.

§Present address: Joint Institute for Heavy Ion Research, Holifield Radioactive Ion Beam Facility, P. O. Box 2008, Building 6008 MS 6374, O.R.N.L. Oak Ridge, TE 37831-6374.

pendent quantity to confirm that the events we will be isolating have flow angle distributions characteristic of fusion-like events.

The multivariate methods we have used need a set of simulations in which both the impact parameter and the source origin are known. To this purpose, we have used the code DIT [13] to create the entrance ^{24}Mg$+^{12}$C channel and the GEMINI code [14] to deexcite the quasiprojectile, quasi-target or the composite system excited nuclei. The simulated events are filtered through the geometrical and energetic cuts of the experimental array and events of total charge equal to or greater than 16 are considered.

An important quantity useful in the determination of cross sections and the classification of nuclear reactions is the impact parameter. This quantity is usually estimated within the help of variables such as the charged-particle multiplicity, the total transverse kinetic energy or the midrapidity charge [15,16]. These methods have proved to be good impact parameter filters for medium or heavy systems characterized with a large range of the observed quantitities, but may not be appropriate for light systems such as the one under study. In the present analysis, we have used, rather than a single variable, a multivariate technique based on a principal component analysis of a large number of observed quantities [3,6]. This technique has been applied to the above-mentioned 26 global variables, V_i and the impact parameter given by the DIT-GEMINI simulations. The best estimate of the impact parameter b_c is obtained as a linear combination of the global variables $b_c = \Sigma_{i=1}^{26} \alpha_i V_i$ that reproduces the impact parameter b given by the simulator with the condition that the linear correlation coefficient between b and b_c is close to unity. The top part of Fig. 1, displaying the estimated impact parameter b_c as a function of the impact parameter for the DIT-GEMINI filtered simulations at 25 MeV/nucleon, shows a nice correlation between the two quantities. The estimated impact parameter for data can then be calculated by using the above linear combination of the V_i. The bottom left part of Fig. 1 which displays the mean value of the charged-particle multiplicity as a function of the estimated impact parameter for data shows the expected relationship between these two quantities. The bottom right part, giving the mean value of the discriminant variable of which low values are associated with fusionlike events as seen below as a function of the estimated impact parameter for data shows a good correlation between these two quantities and also that low impact parameters are associated with low values of D_g. The discriminant variable D_g is obtained by using the discriminant analysis method which gives (in the case of two classes) the best axis that separates the two groups. The top left panel of Fig. 2 displaying the distribution of the simulated discriminant D_g variable obtained as a linear combination of the global V_i variables,

$$D_g = \sum_{i=1}^{26} \beta_i V_i \qquad (1)$$

for one- and two-source events at 25 MeV/nucleon shows that source separation is well achieved. In the simulations,
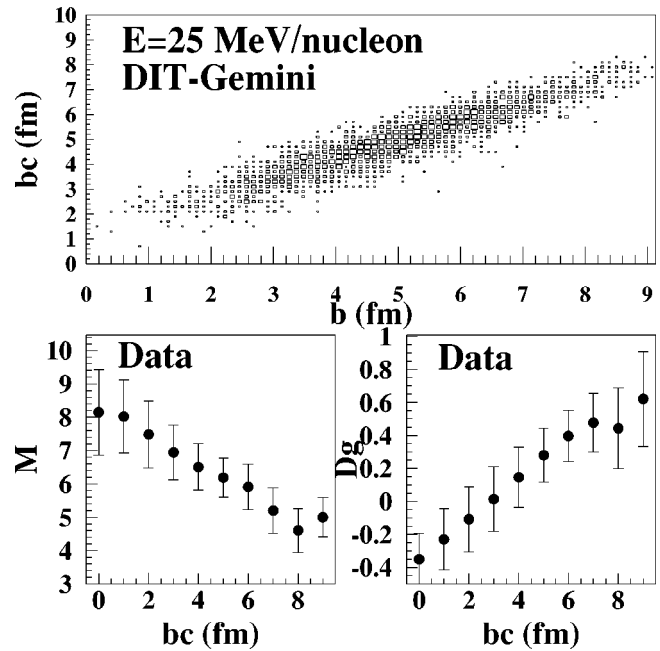

FIG. 1. Top: The estimated impact parameter as a function of the impact parameter for the simulated ^{24}Mg$+^{12}$C at 25 MeV/nucleon events; bottom left: the mean value of the total multiplicity as a function of the impact parameter for data; bottom right: same as left but for the mean value of the discriminant variable.

the cut $D_g \leqslant -0.1$ selects one-source events with a contribution of two-source events less than 10%. Finally, experimental events of which source origin is unknown are projected on this axis and the corresponding D_g distribution is given in the top right corner of Fig. 2. The distribution is disymmetrical and exhibits a two-component structure and can be easily fitted by two Gaussian distributions. The same procedure is
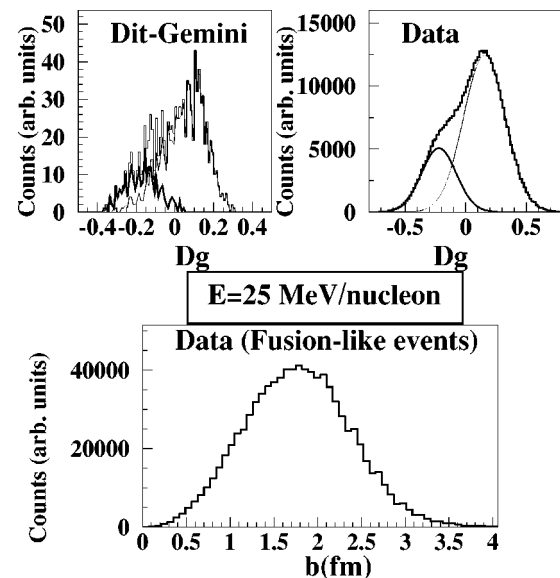

FIG. 2. Top: The discriminant function distribution for simulations (left) and data (right) for the system at 25 MeV/nucleon. The thick (thin) line is the contribution of one- (two-)source events. Bottom: The impact parameter distribution for fusionlike events.

repeated at 35 and 45 MeV/nucleon; yet at these energies the two-component structure is no longer visible, which shows the diminishing importance of fusion with increasing beam energy.

Taking advantage of the "average" one-to-one correspondence between the discriminant variable and the impact parameter shown in Fig. 1, one can obtain a similar relation between D_g and the experimental impact parameter obtained as the geometrical impact parameter distribution corrected for the detection efficiency [3]. This last quantity, which takes account of the geometrical and energetic array limitations and the selection criteria, is determined within the help of the DIT-GEMINI simulations. The impact parameter distributions of fusionlike events is obtained as

$$P_1(b) = P(D_g)\mathcal{I}(b) \quad \text{with} \quad \mathcal{I}(b) = \left(\frac{dD_g}{db}\right)_b \qquad (2)$$

being the Jacobian of the transformation. The bottom part of Fig. 2 gives the resulting impact parameter distribution corrected for detection efficiency for fusionlike events. The fusion cross section is finally computed with formula $\sigma_f = 2\pi\int_0^\infty P_1(b)b\,db$. The computed value is $\sigma = 115 \pm 20$ mb. The uncertainty on this cross section comes mainly from the detection efficiency as this quantity is taken from simulations. This fusion cross section accounts for about 6% of the total reaction cross section as calculated by the parametrization of Kox *et al.* [17]. Such ratios of the fusion cross section to the total reaction cross section are usually reported in the literature for systems of comparable c.m. energy per nucleon. The authors of Ref. [18] have measured a fusion cross section for the system Ni+ Al at 28 MeV/nucleon of about 300 mb which represents 10.2% of the total reaction cross section. Box *et al.* [19] have reported cross section values of 265 mb and 164 mb for the system ^{28}Si+^{28}Si at 26 and 30 MeV/nucleon, respectively, accounting for 11.4% and 6.9% of the total reaction cross section.

Theoretical models used to predict fusion reaction cross sections such as the critical distance model [20] and the Bass model [21] usually divide the c.m. energy range into three regions. These models were developed for low-energy reactions but have been successfully extended to the lower part of the intermediate energy range with the system ^{32}S+^{12}C at 19.5 MeV/nucleon [22]. For the present experiment at 25 MeV/nucleon, the fusion cross section may be evaluated in the higher energy regime of these models in the framework of the critical distance fusion model by the following expression:

$$\sigma_F = \pi d^2\left(1 + \frac{1/2\mu\omega_d^2 d^2 - U_C(d) + Q}{E_{cm}}\right), \qquad (3)$$

where d is the critical distance between the colliding nuclei of reduced mass μ and separation energy Q relative to the compound nucleus. The parameter ω_d is given by $\hbar\omega_d = \beta\omega$ with $\omega = 40A^{-1/3}$ and $\beta = 0.75$. The potential U_C and the critical distance d are defined in Ref. [20]. The model
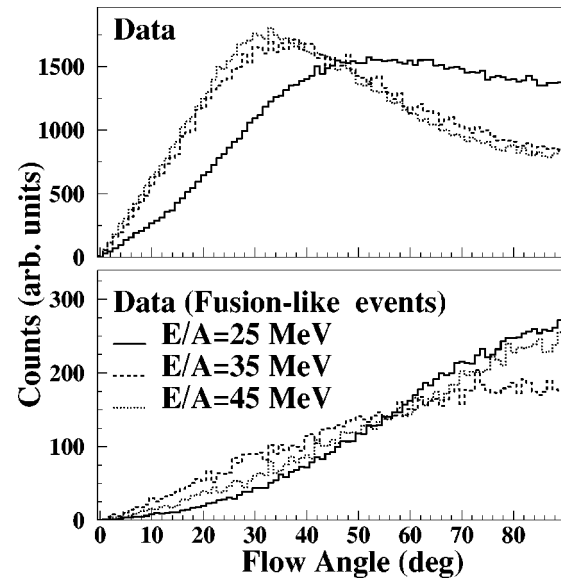

FIG. 3. Top: The flow angle distribution for all $\Sigma Z \geq 16$ events in ^{24}Mg+ ^{12}C reactions at 25, 35, and 45 MeV/nucleon. Bottom: Same as top for selected fusion events. All distributions are normalized to the same number of events.

predicts a fusion cross section for the ^{24}Mg+ ^{12}C at 25 MeV/nucleon of about 500 mb and is larger than the presently measured value. The DIT model we have used predicts fusion up to 3.5 fm which yields a fusion cross section of about 385 mb and is higher than the measured value. Such discrepancies between measured and predicted cross sections in this energy range may be due to the uncertainty on the fusion barriers used in these models. Another fact that can lower the fusion cross section in the ^{24}Mg+ ^{12}C system is the particular alpha structure of the projectile [23] that makes it break up before reaching the critical fusion distance.

The same procedure is repeated for the experiments at 35 and 45 MeV/nucleon and the corresponding fusion cross sections values are found to be 58 and 22 mb, respectively. This observed decrease of the fusion and the increasing importance of other mechanisms such as binary dissipative ones can be seen in the evolution of the flow angle distribution for the three experiments. The top part of Fig. 3 shows the flow angle distribution for the whole data set ($\Sigma_Z \geq 16$) with no selection of the fusion events at the three energies. The distribution at 25 MeV/nucleon has a shape closer to a sinelike pattern typical of one-source events [24,25] than the distribution at 45 MeV/nucleon which has a smaller mean value (45.4° as compared to 54.4° at 25 MeV/nucleon) indicating the fade of fusion and the increasing importance of binary dissipative reactions from 25 to 45 MeV/nucleon.

The fusionlike events are selected by requiring that the discriminant variable be less than −0.1. These events cover a range of estimated impact parameters from 0 to 4 fm as can be seen from Fig. 1. The bottom part of Fig. 3 displays the distribution of flow angle for selected fusionlike events at the three bombarding energies. All distributions are characteristic of single-source events and have high mean values. As the bombarding energy increases, the mean multiplicity first increases from 7.35 at 25 MeV/nucleon to a maximum value of

TABLE I. Relative importance in % for the different fragmenting channels for fusion events and for all events at the three bombarding energies. The numbers between parentheses in the case of fusion events are the cross sections in mb.

Channel	$E/A = 25$ MeV	$E/A = 35$ MeV	$E/A = 45$ MeV
	Fusion events		
1	11.2 (12.9)	10.8 (6.3)	0.2 (0.05)
2	88.3 (101.5)	87.3 (50.6)	81.0 (17.9)
3	0.5 (0.6)	1.5 (0.87)	4.2 (0.93)
4	0.0(0)	0.4 (0.2)	14.6 (3.3)
	All events		
1	4.8	6.9	0.2
2	91.4	89.2	78.2
3	3.6	1.2	11.5
4	0.2	2.7	10.1

7.70 at 35 MeV/nucleon and then decreases to 6.90 at 45 MeV/nucleon. This interesting feature is not due to some trivial detection effects as the GEMINI filtered simulations do not predict this peak in the multiplicity distribution. The values given by these simulations are 6.7, 8.2, and 9.6 for the 25, 35, and 45 MeV/nucleon bombarding energies, respectively. This peak in the multiplicity distribution is neither due to the cut imposed on the discriminant variable as it is also present for the whole complete data set for which the mean values of the multiplicity are 6.85, 7.20, and 6.65 for the three increasing beam energies, respectively. In order to understand the origin of this peak in the multiplicity distribution, the different decay channels were classified into four categories. (i) A class containing only light charged particles (LCP's, $Z = 1,2$). (ii) A class with one or two IMF's and LCP's and no residue. (iii) A multifragmentation class with three or more IMF's and LCP's. (iv) A class with a heavy residue ($Z \geq 10$) and IMF's or LCP's.

Table I gives the relative importance of these different decay channels for fusion events (also given in this case the cross sections in mb) and for all events at the three bombarding energies. A striking feature is the disappearance of the decay channel with only LCP's at 45 MeV/nucleon and the growing importance of the multifragmentation channel. At 25 MeV/nucleon, when considering only the $\Sigma Z = 18$ events, the most abundant LCP's channels are the 8He2H and 7He4H channels and account for 6.5% and 1.7%, respectively, of all 343 ^{36}Ar possible breakup channels. The total number of breakup channels, is calculated from multiplicity 3 to 12 and with the condition that the maximum detected charge is 12. At 35 MeV/nucleon the former LCP's channels account for 3.8% and 5.4% respectively. The contribution of both these channels to all channels at 45 MeV/nucleon is very low and only about 0.1%. As the decay channels with only LCP's are characterized with high multiplicities (10 and 11), their absence at 45 MeV/nucleon is responsible for the observed decrease of the total multiplicity at this energy. This rise and fall of the multiplicity is usually observed for fragments and intermediate mass fragments for heavy or medium mass systems [26–34]. Some recent quantum molecular dynamics Ca-Ca simulations [35] have shown that the

peak in fragment production can be related to the onset of multifragmentation. For very light systems as the one under study presently and to our knowledge, it is the first observation of the rise and fall of the total charged-particle multiplicity. It may seem paradoxal that with the increase of beam energy, class 1 which we may call "vaporization" will disappear. True vaporization occurs when the system promptly disintegrates into its elemental constituents with atomic numbers less than 3 and is expected to occur around an excitation energy of 6 MeV/nucleon [36]. This does not seem to be the case in this particular small system. The picture that can be drawn here is that at 25 and 35 MeV/nucleon, the system may undergo full deexcitation sequential steps leading finally to a channel with only light charged particles. At 45 MeV/nucleon, the excitation energy increases and the multifragmentation decay mode opens. When considering the $\Sigma Z = 18$ system, channels with as much as five IMF's such as B+4Li+H, 5Li+He+H, Be+4Li+2H, and B+Be+3Li are observed and represent 0.2% of all possibilities. Channels with three, four, or five IMF's are all produced with a comparable yield, each one less than 0.5%, with the exception of channels C+Be+Li+He+3H, C+2Li+2He+2H, C+B+Li +He+2H, and C+Be+Li+2He+H which yield represents between 0.5% and 1% of all yields. The total number of these open fragmentation channels is 98 while at 25 and 35 MeV/nucleon it is only 21 and 32, respectively. Energy threshold effects cannot account for this as the center-of-mass velocity even at 25 MeV/nucleon is higher than the energy thresholds. Moreover, if these effects were important, they should also favor the production of $Z = 2$ particles at 45 MeV/nucleon which is not the case as we have seen above. In a recent study [4], we have constructed two-fragment reduced velocity correlation functions and showed that this class (here called 3) of events (which we labeled C in that study) is associated with a short time scale suggestive of prompt multifragmentation. Another interesting fact at 45 MeV/nucleon is the importance of class 4 characterized by a copious production of a heavy residue ($Z \geq 10$) and one IMF. This class of events has been also attributed to fusionlike events by a discriminant analysis applied to the 625 quadrimoments [4] and labeled class A in that work. These events have been attributed to the formation of an orbiting dinuclear system that reseparates after a short time.

In conclusion, we have selected in this work fusionlike events in the ^{24}Mg$+ ^{12}$C system at three bombarding energies of the intermediate energy domain by applying the discriminant analysis method to a set of 26 global variables. The measured fusion cross sections are found to be lower than theoretical values and to decrease strongly with increasing beam energy. The total charged-particle multiplicity presents a peak at 35 MeV/nucleon which may indicate the appearance of a change in the decay mechanisms. The sequential evaporative decay at 25 MeV/nucleon leading to channels containing only LCP's is strongly suppressed at 45 MeV/nucleon and is replaced by the multifragmentation decay mechanism that opens strongly and competes with the more traditional decay channels such as particle or light fragment evaporation and orbiting.

[1] C.K. Gelbke and D.H. Boal, Prog. Part. Nucl. Phys. **19**, 3 (1987).

[2] L.G. Moretto and G.J. Wozniak, Annu. Rev. Nucl. Part. Phys. **43**, 397 (1993).

[3] P. Désesquelles *et al.*, Phys. Rev. C **62**, 024614 (2000).

[4] M. Samri *et al.*, Nucl. Phys. **A700**, 42 (2002).

[5] Y. Larochelle *et al.*, Phys. Rev. C **53**, 823 (1996).

[6] A. M. Maskay-Wallez, Ph.D. thesis, Université Claude Bernard I, 1999.

[7] O. Lopez *et al.*, Phys. Lett. B **315**, 34 (1993).

[8] R. Bougault *et al.*, Nucl. Phys. **A488**, 255c (1988).

[9] C.G. Fox and S. Wolfram, Phys. Rev. Lett. **41**, 1581 (1978).

[10] A. D. Nguyen, Ph.D. thesis, Université de Caen, 1998.

[11] J. Cugnon and D. L'Hote, Nucl. Phys. **A397**, 519 (1983).

[12] H. Strobele *et al.*, Phys. Rev. C **27**, 1349 (1983).

[13] L. Tassan-Got and C. Stéphan, Nucl. Phys. **A524**, 121 (1991).

[14] R.J. Charity *et al.*, Nucl. Phys. **A476**, 516 (1988).

[15] J. Péter *et al.*, Nucl. Phys. **A519**, 611 (1990).

[16] L. Phair *et al.*, Nucl. Phys. **A458**, 489 (1992).

[17] S. Kox *et al.*, Nucl. Phys. **A420**, 162 (1984).

[18] L. Lebreton *et al.*, Eur. Phys. J. A **3**, 325 (1998).

[19] P.F. Box *et al.*, Phys. Rev. C **50**, 934 (1994).

[20] T. Matsuse *et al.*, Phys. Rev. C **26**, 2338 (1982).

[21] R. Bass, Phys. Rev. Lett. **55**, 265 (1977).

[22] S. Pirrone *et al.*, Phys. Rev. C **64**, 024610 (2001).

[23] A.H. Wuosmaa *et al.*, Phys. Rev. Lett. **68**, 1295 (1992).

[24] L. Beaulieu *et al.*, Phys. Rev. Lett. **77**, 462 (1996).

[25] Y. Larochelle *et al.*, Phys. Rev. C **62**, 051602(R) (2000).

[26] C.A. Ogilvie *et al.*, Phys. Rev. Lett. **67**, 1214 (1991).

[27] M.B. Tsang *et al.*, Phys. Rev. Lett. **71**, 1502 (1993).

[28] R.T. Souza *et al.*, Phys. Lett. B **268**, 6 (1991).

[29] G.F. Peaslee *et al.*, Phys. Rev. C **49**, R2271 (1994).

[30] C. Williams *et al.*, Phys. Rev. C **55**, R2132 (1997).

[31] T. Li *et al.*, Phys. Rev. Lett. **70**, 1924 (1992).

[32] K. Hagel *et al.*, Phys. Rev. Lett. **68**, 2141 (1992).

[33] N.T.B Stone *et al.*, Phys. Rev. Lett. **78**, 2084 (1997).

[34] B. Jakobsson *et al.*, Nucl. Phys. **A509**, 195 (1990).

[35] Rajeej K. Pur and Suneel Kumar, Phys. Rev. C **57**, 2744 (1998).

[36] M.F. Rivet *et al.*, Phys. Lett. B **388**, 219 (1996).